

PAPER

Bioinspired algorithm for autonomous sensor-driven guidance in turbulent chemical plumes

To cite this article: D R Webster *et al* 2012 *Bioinspir. Biomim.* **7** 036023

View the [article online](#) for updates and enhancements.

Related content

- [Numerical simulations of odorant detection by biologically inspired sensor arrays](#)
R Schuech, M T Stacey, M F Barad *et al.*
- [Effects of sensilla morphology on mechanosensory sensitivity in the crayfish](#)
Swapnil Pravin, DeForest Mellon Jr, Edward J Berger *et al.*
- [Odor-conditioned rheotaxis of the sea lamprey: modeling, analysis and validation](#)
Jongeun Choi, Soo Jeon, Nicholas S Johnson *et al.*

Recent citations

- [3D Moth-inspired chemical plume tracking and adaptive step control strategy](#)
Bo Gao *et al*
- [Multi-agent search for source localization in a turbulent medium](#)
Hadi Hajieghrary *et al*
- [Autonomous tracking of chemical plumes developed in both diffusive and turbulent airflow environments using Petri nets](#)
Jie Yuan *et al*

Bioinspired algorithm for autonomous sensor-driven guidance in turbulent chemical plumes

D R Webster¹, K Y Volyanskyy¹ and M J Weissburg²

¹ School of Civil & Environmental Engineering, Georgia Institute of Technology, 790 Atlantic Drive, Atlanta, GA 30332, USA

² School of Biology, Georgia Institute of Technology, 310 Ferst Drive, Atlanta, GA 30332, USA

Received 24 February 2012

Accepted for publication 6 June 2012

Published 25 June 2012

Online at stacks.iop.org/BB/7/036023

Abstract

We designed and implemented a control algorithm for sensor-mediated chemical plume tracking in a turbulent flow environment. In our design, we focused on development of a signal processing strategy capable of replicating behavioral responses of actively tracking blue crabs (*Callinectes sapidus*) to chemical stimuli. The control algorithm is evaluated in a hardware platform that allows motion in two directions (i.e. forward–back and left–right). The geometric arrangement of the sensor array is inspired by the location of blue crab sensor populations. Upstream motion is induced by a binary response to supra-threshold spikes of concentration, and cross-stream steering is controlled by contrast between bilaterally-separated sensors. Like animal strategies, the developed control algorithm is dynamic. This property allows the algorithm to function effectively in the highly irregular turbulent environment and produces adaptive adjustments of motion to minimize the distance to the source of a plume. Tracking trials indicate that roughly 80% of the tracks successfully stop near the plume source location. Both success rate and movement patterns of the tracker compare favorably to that of blue crabs searching for odorant plume sources, thus suggesting that our sensory-mediated behavior hypothesis are generally accurate and that the associated tracking mechanisms may be successfully implemented in hardware.

1. Introduction

Our goal is to develop a feedback control algorithm to autonomously track turbulent chemical plumes and locate the plume source with a high degree of success and low rate of false detection. To accomplish this goal, we draw inspiration from the success of mobile benthic organisms, in particular blue crabs (*Callinectes sapidus*). Chemosensation is an important sensory mode for many crustaceans, allowing them to locate food, mates, or predators (Breithaupt and Thiel 2011), so these animals represent effective strategies. Major challenges in understanding (and mimicking) chemosensory-mediated guidance are to quantify the characteristics of the relevant chemical signal structure that provide information and how this information is used to mediate movement to the source. Our extensive studies of chemosensory navigation (Keller *et al* 2003, Jackson *et al* 2007, Page *et al* 2011a, 2011b)

have provided a series of potential schemes by which animals encode and respond to chemical information, some of which we have implemented in an autonomous tracking system. This allows us to test hypothesized mechanisms of animal behavior while simultaneously examining whether such mechanisms can be used for autonomous guidance.

In contrast to the high performance displayed by animals, we have yet to develop good tracking strategies for use in autonomous vehicles that track turbulent chemical plumes. Traditional sensing approaches, such as time-integration to compute average properties, fail in turbulent plumes due to the high spatial and temporal variability of the chemical signal. Nevertheless, there have been numerous attempts at chemically-mediated tracking strategies (reviewed by Nakamoto *et al* 1999, Russell 2001, Lilienthal *et al* 2006, Kowadlo and Russell 2008), mostly inspired by analysis or observation of animal behavior. The best strategies use some



Figure 1. Flow visualization of the chemical plume, which is created via a continuous iso-kinetic release of a dye solution into a fully developed turbulent boundary layer. The view is from above, with the flow moving from left to right.

of the principles employed by animals, especially terrestrial and aquatic arthropods (i.e. moths and blue crabs or lobsters), which have developed sensing mechanisms that are well-matched to the properties of turbulent chemical plumes.

Using our understanding of turbulent scalar field characteristics, information content in chemical plumes, and chemically-mediated behavior of animals, we developed and tested a sensor-mediated algorithm for tracking chemical plumes. To this goal, we developed a test bed to facilitate the evaluation of the general feedback control mechanisms that enable effective tracking using information from turbulent chemical plumes. Consistent with crustacean observations and inspiration, the spatial scale of these tracking processes are on the order of meters and the temporal scale is on the order of tens of seconds.

2. Background

This section reviews animal strategies for extracting information from the plume structure in order to move successfully toward the source. The basic question is: what information in the intermittent and chaotic plume structure is providing cues to guide tracking?

2.1. Information in turbulent chemical plumes

Figure 1 shows a photograph of a chemical plume in a turbulent water flow. The effluent has been released from a small orifice at the upstream (left) edge of the photograph. The filament forms an irregular pattern that wanders randomly across the image, which is evidence of the turbulent stirring process. The concentration within the filament is clearly more dilute in some regions compared to others, and the concentration distribution shows a complex pattern in space, which is continually evolving. The characteristics of odorant plumes in such environments cannot be predicted via analytical methods (e.g., turbulent diffusivity models) or simple numerical simulations. However, advances in experimental technology have provided valuable quantitative insight to the spatial and temporal variation of chemical plumes in the aquatic turbulent environment (e.g., Webster and Weissburg 2001, Crimaldi *et al* 2002). For instance, laser-induced fluorescence (LIF) is an optical measurement technique that yields sequences of the

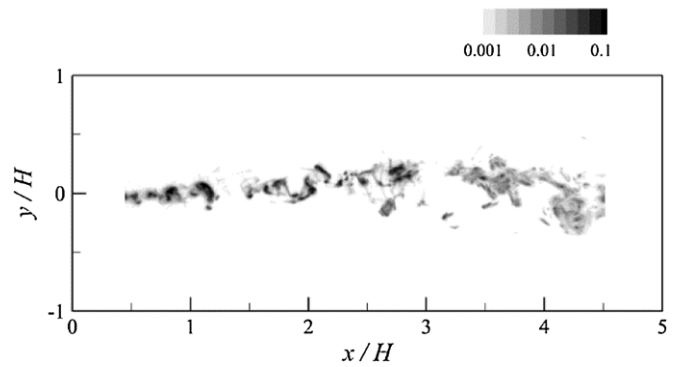


Figure 2. A sample instantaneous concentration field. The chemical source is located at $x = 0$ and $y = 0$ and the release is iso-kinetic into a fully-developed turbulent boundary layer. The flow direction is in the positive x -direction. H is the channel depth and equals 20 cm. The contour values are normalized by the source concentration (i.e., c/C_0).

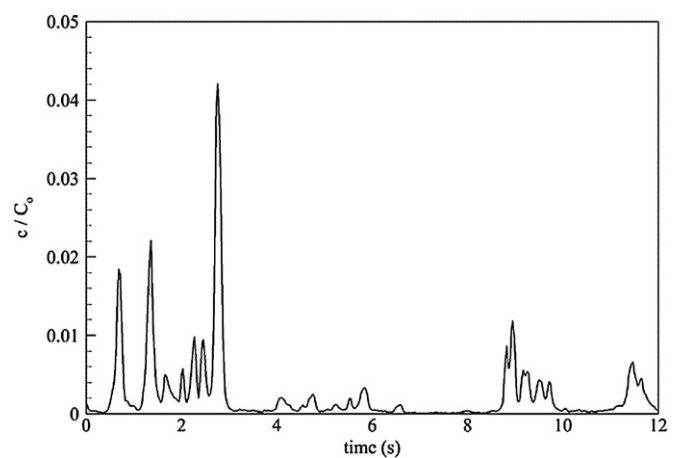


Figure 3. Sample time record of concentration at a point along the plume centerline. The instantaneous concentration is normalized by the source concentration.

instantaneous concentration spatial distribution (Webster *et al* 2003; also figure 2). Such visualization methods demonstrate the significant spatial variation in the chemical plume structure. Further, the instantaneous structure of the concentration field is continuously evolving in time as demonstrated by the example time record at a point (shown in figure 3).

The smooth and predictable gradient in the time-averaged concentration field (figure 4) suggests a useful tracking strategy would be to move up the concentration gradient by sequentially comparing the response of a single sensor to advance in the direction of increasing concentration (i.e. klinotaxis). Small organisms, such as bacteria and nematodes, are believed to employ this strategy in laminar flow environments (reviewed in Webster and Weissburg 2009). Unfortunately, this strategy is ineffective for rapid tracking of turbulent chemical plumes for the simple reason that the information shown in figure 4 is unavailable to the tracker. The time period necessary to determine the time-averaged concentration at a single point with sufficient accuracy to perceive the gradient direction is many minutes (Webster and Weissburg 2001). Rapidly mobile trackers, such as blue crabs, are observed to track distances of roughly 2 m in 30 s or

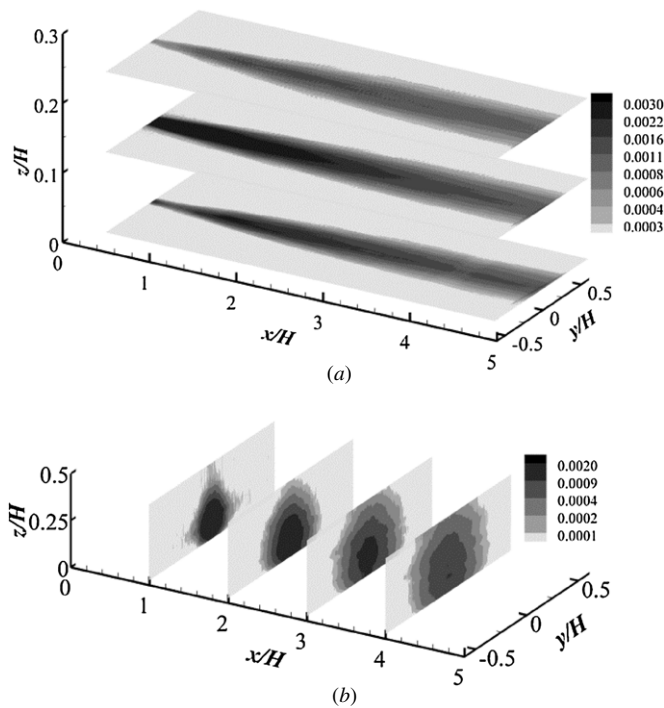


Figure 4. Time-averaged concentration field. (a) Contours shown in horizontal (x - y) planes at elevations $z/H = 0.029, 0.145, 0.26$. (b) Contours shown in vertical (y - z) planes at distances $x/H = 1.0, 2.0, 3.0,$ and 4.0 . The chemical source is located at $x = 0$ and $y = 0$ and the release is iso-kinetic into a fully-developed turbulent boundary layer. The flow direction is in the positive x -direction. H is the channel depth and equals 20 cm. The contour values are normalized by the source concentration (i.e. \bar{c}/C_0).

less, which is inconsistent with a slow sampling strategy that compares time-averaged concentration values. It is clear that blue crabs, and other organisms such as insects, are employing strategies that are much more efficient than waiting for time-averaged quantities to statistically converge (e.g., Weissburg and Zimmer-Faust 1994, Vickers 2000, Kozłowski *et al* 2003, Gardiner and Atema 2007). Thus, they appear to be acquiring information from the fluctuating plume structure.

2.2. Tracking strategies

Blue crabs use input from two sets of chemosensors that are processed in parallel to regulate tracking behavior (Keller *et al* 2003, Page *et al* 2011a, 2011b), and do so by taking advantage of chemical plume structure at different elevations in the water column (Jackson *et al* 2007, also see Reidenbach and Koehl 2011). Chemosensors on the antennules, which are elevated on the blue crab's body, control the forward movement of the blue crab via odor-gated-rheotaxis (a strategy whereby odorant arriving at these sensors is coupled with mechanosensory information of water movement (i.e. sensing flow direction) to induce upstream motion towards the odorant source. Chemosensors on the crab's legs, which are spatially separated and near the substrate, are believed to mediate cross-stream motion relative to the plume structure. Although these two sensor populations largely regulate different aspects of behavior, information from both populations also interact in specific circumstances. The combination of sensors at different

heights in the water column means that blue crabs are acquiring time-varying, three-dimensional (3D) information about their environment.

Extensive experiments in which we simultaneously visualized chemical signal structure using three-dimensional laser-induced fluorescence (3DLIF) and animal movements (Dickman *et al* 2009) suggest that chemical stimuli elicit responses in a binary fashion by causing upstream motion provided the concentration at the antennules exceeds a specific threshold (Page *et al* 2011a). Thresholds are different for each crab, indicating a physiologically context-sensitive response to signal dynamics. The mean time period that it takes blue crab to reach above-average velocity following a supra-threshold antennule spike is in the range of 0.4–0.6 s (Page *et al* 2011a). Our data also indicate that high frequency of chemical spike encounters terminates upstream movement, but again, animals in different environmental conditions use different frequency thresholds. Further, the data provide evidence that the previous state of the animal and prior stimulus history influence the behavioral response (i.e. the response is physiologically context dependent (Page *et al* 2011a)). First, crabs receiving prior chemical spikes attain elevated velocity more quickly in response to subsequent spikes. Prior spikes occurring at leg or antennule sensors produce this response, showing how information from multiple sensor populations interacts. Second, prior acceleration or deceleration of the blue crab influences the response time period to a particular chemical spike; blue crabs that are accelerating respond to chemical spikes more quickly than those that are not.

The 3D concentration fields also facilitate a consideration of the role of broadly-distributed sensor populations in chemosensory searching, especially cross-stream heading adjustment. The spatial distribution of the chemical concentration field is necessary and sufficient to mediate correct cross-stream motion, although concentration magnitude provides information that supplements that obtained from the spatial distribution (Page *et al* 2011b). Crabs detect and respond to shifts in the cross-stream position of the center-of-mass of the chemical concentration distribution as small as 5% of the leg span, which corresponds to roughly 0.8–0.9 cm. The reaction time after an above threshold shift in the position of the center-of-mass is in the range of 2–4 s. The data also indicate that these steering responses are dependent on stimulus history or other characteristics of the plume, with animals taking longer to respond in environmental conditions with large-scale spatial meanders (Page *et al* 2011b).

3. Methods and materials

We elected to test refined algorithms inspired by blue crabs tracking behavior using real sensor arrays exposed to turbulent chemical plumes in a controlled hydrodynamic environment. Experimental trials were conducted in a 1.07 m wide, 24 m long tilting flume. A submerged pump delivered water to the head box of the tilting flume from an underground sump. Stilling devices in the head box conditioned the flow entering the flume to be spatially uniform with low turbulence intensity.

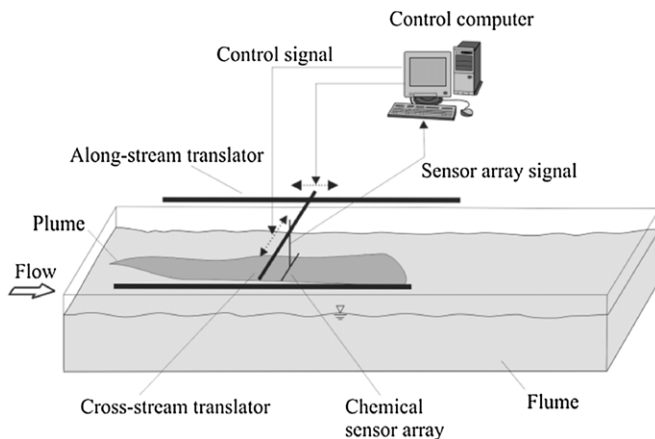


Figure 5. Sketch of the algorithm-testing apparatus. The two-axis linear translator system is interfaced to the control computer, which acquires signals from a three-sensor-array.

The tailgate position and bed slope were adjusted to create uniform depth flow conditions (flow depth $H = 20$ cm). For the measurements reported here, the average channel velocity, U , was 5 cm s^{-1} . The boundary layer characteristics for these flow conditions were previously reported in Rahman and Webster (2005).

The tracking system processes chemical sensor signals and autonomously moves the sensor array (figure 5). The system allows us to focus on developing sensing strategies (as opposed to drive-train control) by avoiding implementation on a fully-autonomous mobile robotic platform. Note that a similar approach was taken in the wind tunnel trials of Rutkowski *et al* (2004) and Edwards *et al* (2005) who employed a robotic gantry apparatus in order to implement tracking algorithms in a hardware platform. In the current study, the motor actuators, which consist of linear translators, allow independent motion in two directions. The linear translator system was constructed by Parker automation and consists of motor-driven rodless actuators aligned with the along-stream and cross-stream directions (figure 5). The motor controllers accept command strings to guide their motion. The cross-stream span of the system is 1 m, and the along-stream length is 2 m, with actuator speeds that allow the device to move at rates of up to 15 cm s^{-1} (equivalent to blue crabs). For the trials reported herein, the command speed was preset at 6.1 cm s^{-1} in the along-stream direction and 3 cm s^{-1} in the cross-stream direction. The step size is 10 cm in the along-stream direction and 5 cm in the cross-stream direction. The system does not include a flow sensor. Rather, the flow direction is assumed based on the constraints of the channel flow.

We employ fast conductivity sensors (Precision Measurement Engineering, Inc.) to develop tracking algorithms because they provide spatial (0.5 mm) and temporal (up to 800 Hz) resolution that allows us to replicate animal capabilities. The plume source consists of a neutrally-buoyant salt (NaCl) water solution released into the fully developed turbulent boundary layer via a small (4.2 mm diameter) nozzle (NaCl concentration is 47 g l^{-1} and isopropyl alcohol is added to the salt solution to create neutral buoyancy). The

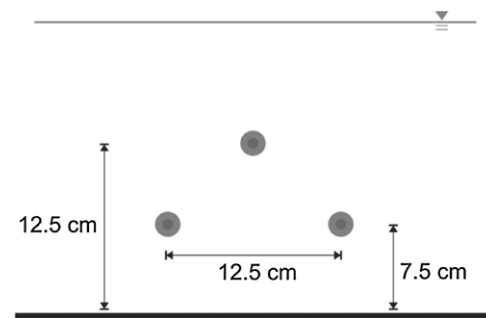


Figure 6. Sketch of sensor array geometry.

release nozzle is located 3.8 cm above the flume bed with the iso-kinetic release (i.e. 5 cm s^{-1}) pointed downstream. This duplicates previous methods, hence provides a well understood chemical stimulus environment (e.g., Webster and Weissburg 2001, Webster *et al* 2003, Rahman and Webster 2005) in which to test our sensor-mediated strategies and facilitates comparisons with blue crabs tested in the same environmental conditions (e.g., Keller *et al* 2003, Jackson *et al* 2007, Page *et al* 2011a, 2011b). The arrangement of the three conductivity sensors is inspired by the geometric arrangement of the antennule and leg chemosensors on blue crabs. Two sensors are broadly separated in the cross-stream direction (12.5 cm separation) and positioned 7.5 cm above the flume bed (figure 6). The cross-stream separation distance mimics that of blue crabs, and we note that Grasso *et al* (1996) employed cross-stream sensor separation distances in the range of 1 to 9 cm in their lobster-inspired robot. The third sensor is located higher (12.5 cm) above the flume bed and is centered in the cross-stream direction (figure 6).

The sensor signal (output as voltage) is collected by the control computer and applied to the rule-based tracking algorithm (described below) that commands the linear translators to move the sensor array. The analogue-to-digital signal collection is performed with a multi-purpose DAQ module with 8 A/D (range -5 to 5 V) channels available (National Instruments). Sensor data were collected at 20 Hz, which provided a good balance between rapid sample update rate and minimizing signal noise. The data acquisition and tracking algorithm is programmed in MATLABTM. Commands are sent to the linear translator controllers via Ethernet Communication Interface and are initiated by a C++ code (which interfaces with the primary MATLABTM code).

4. Description of tracking algorithm

Improvements on previous approaches to autonomous chemically-mediated guidance in turbulent plumes are necessary, and possible, given the existing information reviewed above. The sensor-mediated tracking algorithm (figure 7) consists of the following elements:

- *Data acquisition unit*—acquires chemical signal information.
- *Relative position/data builder*—acquires and records position of the tracker.

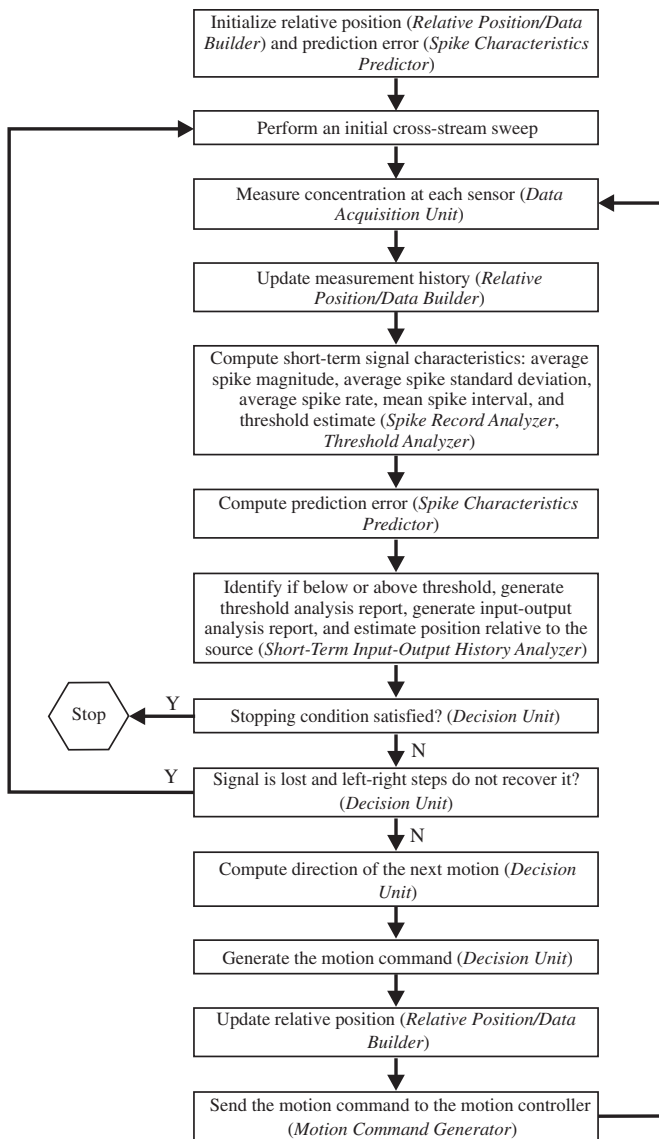


Figure 7. Flow chart of the sensor-driven control algorithm.

- *Spike record analyzer*—quantifies spike characteristics.
- *Threshold analyzer*—determines current spike thresholds relative to previous thresholds.
- *Spike characteristics predictor*—predicts future spike magnitude.
- *Short-term input–output history analyzer*—examines spike threshold comparisons to specify movement.
- *Decision unit*—integrates the information to prescribe the next motion.
- *Motion command generator*—generates motion commands to hardware.

During operation, the tracker performs upstream and cross-stream motions in search of the direction of the spike magnitude increase. The purpose of the *relative position/data builder* is to construct a data map of the performed motions and corresponding measurements and store these data in the long-term memory. Motion commands depend on the estimation of spike sequence characteristics (spike magnitude, spike standard deviation, spike frequency, mean inter-spike interval,

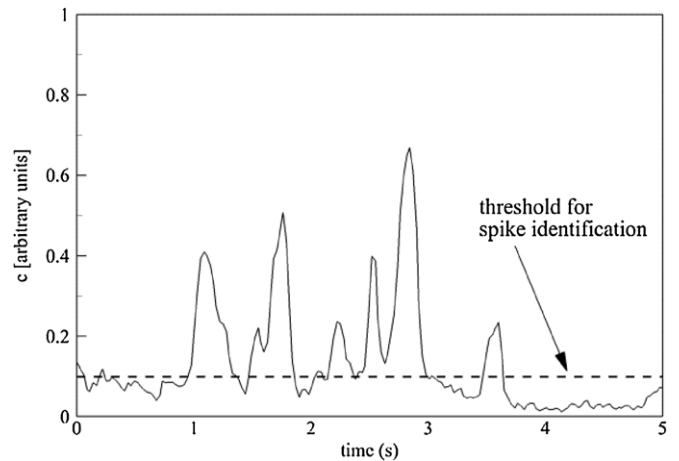


Figure 8. Example time record of the sensor signal with a threshold for spike identification shown. Spikes are defined as local maxima that exceed the threshold. Local maxima below the threshold are not included in the algorithm processing.

and current stage of motion) performed by the *spike record analyzer*. The search algorithm is based on a binary threshold paradigm we observe in blue crabs; the threshold is estimated adaptively during the search process by the *threshold analyzer*. The *spike characteristics predictor* uses short-term (2–10 s) memory data to predict the characteristics of a one-step-ahead measurement. The *spike characteristics predictor* output is used to compute a prediction error which is sent to the *short-term input–output history analyzer* and subsequently used in the *decision unit*. Motion commands are generated and sent to the motion control system by a combination of the *decision unit* and *motion command generator*. The *decision unit* maps the input signal pattern to the appropriate class of response replicating the likely response of a blue crab. This is required since we use variable threshold rules inspired by our analysis of blue crab tracking, hence information on movement history and current position enables us to employ these rules based on the current position of the sensor platform.

The *spike record analyzer* governs the critical step of analysis of the incoming odorant signal. This element first defines a spike as any sample in the record for which the two neighboring samples (i.e. previous and next) have smaller magnitude. During data processing and spike identification, a minimum threshold value of -4.98 V is applied to exclude noise from subsequent analysis (recall that voltage signal range is -5 – $+5$ V). Thereafter, a dynamic threshold value is computed based on $C_{avg}/2$ rule (see Page *et al* 2011a), which consists of defining the threshold based on half of a running average of the spike concentration values. Only spikes that exceed this threshold value are considered in further analysis (see figure 8).

Upstream motion is governed by the analysis of the short-term history of the concentration measurements (*short-term input–output history analyzer* and *decision unit*). Together, these two modules, compare current odor spikes to the average spike magnitude of the previous step, and then determine the subsequent motions. ‘Average’ means time average over the period since the previous step, and the center probe has

greater weighting for this function compared to the other probes, which is consistent with our observations of blue crabs (Keller *et al* 2003, Page *et al* 2010a). The current average spike magnitude is compared to the previous value for this evaluation, and forward motion is prescribed (by the *decision unit*) when the current magnitude exceeds the previous value. We initially tested three conditions: (1) comparison to 90% of the previous value, (2) comparison to previous value, and (3) comparison to 110% of the previous value. Condition (1) resulted in frequent loss of the plume as the tracker moved forward but off from the plume's main axis, whereas (3) resulted in more frequent stops and trajectory oscillations in response to perceived signal decrease.

Further, if the current average spike magnitude is less than the previous value, it is compared with the predicted value obtained from the *spike characteristics predictor*. If the prediction error (i.e. predicted value minus the average spike magnitude) is small (less than 2%), then upstream motion is activated, otherwise cross-stream movement occurs in response to perceived signal loss (± 5 cm; initial direction follows from bilateral signal contrast), and analyzes the spikes observed. If the prediction error is large at the neighboring locations, the tracker moves to the leftmost position and initiates a full cross-stream sweep to re-acquire the plume signal. In addition, after each full cross-stream sweep (initial or when plume signal is lost) and corresponding identification of the cross-stream position with the greatest concentration signal, the tracker moves one step upstream relative to the location of that position. Finally, the stopping criterion is based on exceeding a threshold frequency of concentration spikes, which is computed by the *short-term input-output history analyzer*, and acted upon by the *decision unit*. The threshold is set at 2 Hz based on information from blue crab trials.

Control of cross-stream motion is essential for plume tracking, since correct identification of the cross-stream direction of greater concentration helps the tracker maintain contact with the plume (Zimmer-Faust *et al* 1995, Weissburg and Dusenbery 2002, Jackson *et al* 2007). A cross-stream sweep is performed in the initial step (first tracker motion) to locate the plume, which is analogous to the tendency of animals to move cross-stream in order to initiate or regain contact with the odorant plume. Thereafter, cross-stream steering is accomplished by the steering module (within the *decision unit*) with or without simultaneous along-stream motion at each step. The cross-stream motion is directed by the steering algorithm based on the contrast of the spikes detected on the two steering probes (leftmost and rightmost probes). The algorithm defines a parameter that specifies a minimum percentage difference in peak concentration that is required to move cross-stream toward the side with the higher value. For the trials reported below, the minimum difference parameter is set at 30%.

The cross-stream and along-stream motions are integrated, which requires a situation-dependent balance of the motion commands, which is determined by the *decision unit*. This is inspired by our observations that blue crabs do not always move upstream in response to signal, suggesting they perform such a physiologically context sensitive weighting

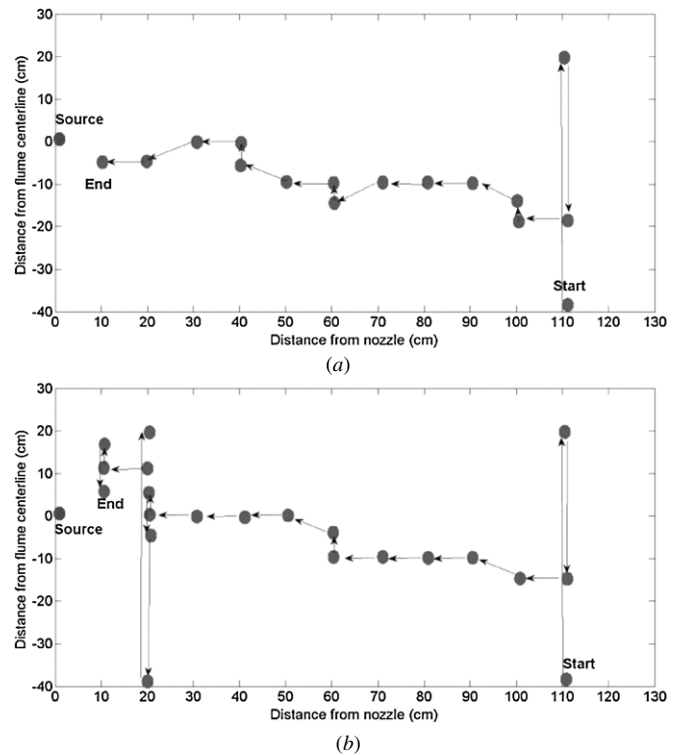


Figure 9. Two (typical) examples of successful sensor-mediated tracks to the plume source. The time period of each step is typically 3.5 s. The full cross-stream sweeps take longer, roughly 20 s.

of signals mediating upstream versus cross-stream motion. Along-stream motion is performed simultaneously with the cross-stream motion if the average recorded peak value at the current step is larger than at the previous step. Alternatively, only the cross-stream motion is performed if the average recorded peak value at the current step is smaller.

5. Results

Figure 9(a) shows an example of a successful track performed by the sensor-equipped tracker. The tracker initially performs a complete cross-stream sweep. It then returns to the identified location of the greatest peak concentration and makes one step forward. The tracker performs subsequent autonomous along-stream and cross-stream motions by following the rule-based algorithm described above. The tracker autonomously stops close to the source when the spike frequency reaches the 2 Hz threshold. Figure 10 shows two arbitrarily-selected, but typical, blue crab tracks that successfully located the source. The autonomous track shown in figure 9(a) visually compares very well with the blue crab track shown in figure 10(a) in terms of directness to the source.

Figure 9(b) shows a second example track performed by the autonomous sensor-driven tracker. In this example, the tracker loses contact with the sensory cue at roughly 20 cm downstream of the source location, and after failing to re-acquire with a step to the right and a step to the left the tracker performs a full cross-stream sweep. The trajectory near the source is far from direct, but the tracker does eventually autonomously stop near the source. Again, comparison with

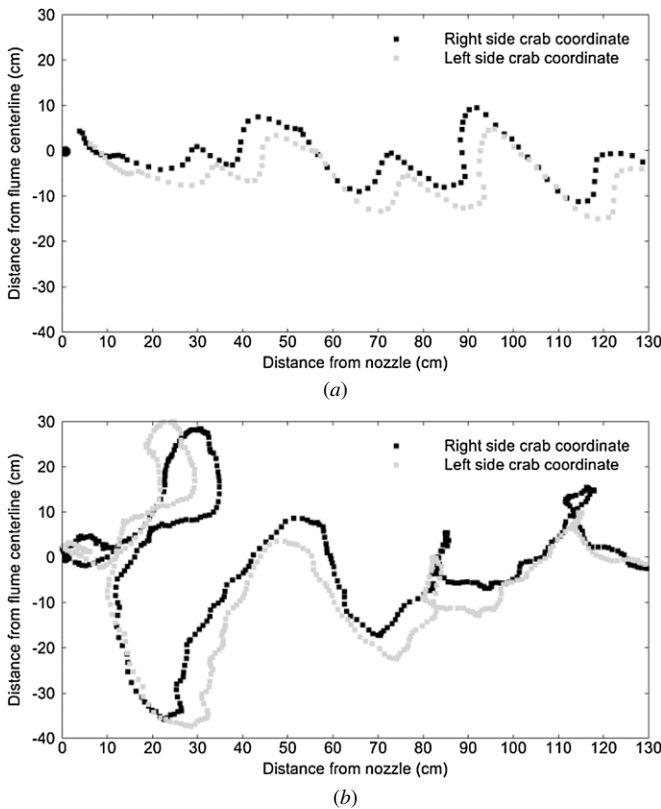


Figure 10. Two (typical) examples of successful blue crab tracks to the plume source. The symbols indicate the location of a pair of LED lights in battery-powered backpack on the carapace of the crab. The time period between neighbouring symbols is 0.2 s.

a sample blue crab track (figure 10(b)) reveals that animal trackers also on occasion include large cross-stream motions near the source.

Forty-three trails were performed with the plume characteristics defined above. For each trial, the initial distance of the tracker from the source was 114 cm. Of these trials, 35 tracks (81%) are declared as successful at autonomously moving toward the source and stopping in near proximity. The average final distance from the plume source location for the successful trials is 14.3 cm.

We analyzed the tracking kinematics of the 17 successful search tracks for which we also recorded the tracker position through time. The mean tracking period is 75 ± 17 s including 20 s corresponding to the initial full cross-stream sweep. The tracker averaged roughly 3 cm s^{-1} over the duration of the search. Overall, the search trajectory was efficient; the ratio of the straight line distance from the initial tracker position to the total distance traveled (NGDR, or net-to-gross-displacement-ratio) averaged 0.7 ± 0.03 (mean \pm std. err.). As suggested by figure 9(a), quantitative analysis of the successful tracks showed that the tracker moved more quickly, and converged onto the plume centerline as it approached the source. When the tracker was in the range of 100–50 cm downstream of the source, the movement velocity was slower by roughly 0.4 cm s^{-1} and the distance from the centerline was more than 6 cm greater than the quantities in the range of 50–0 cm from the source (figure 11).

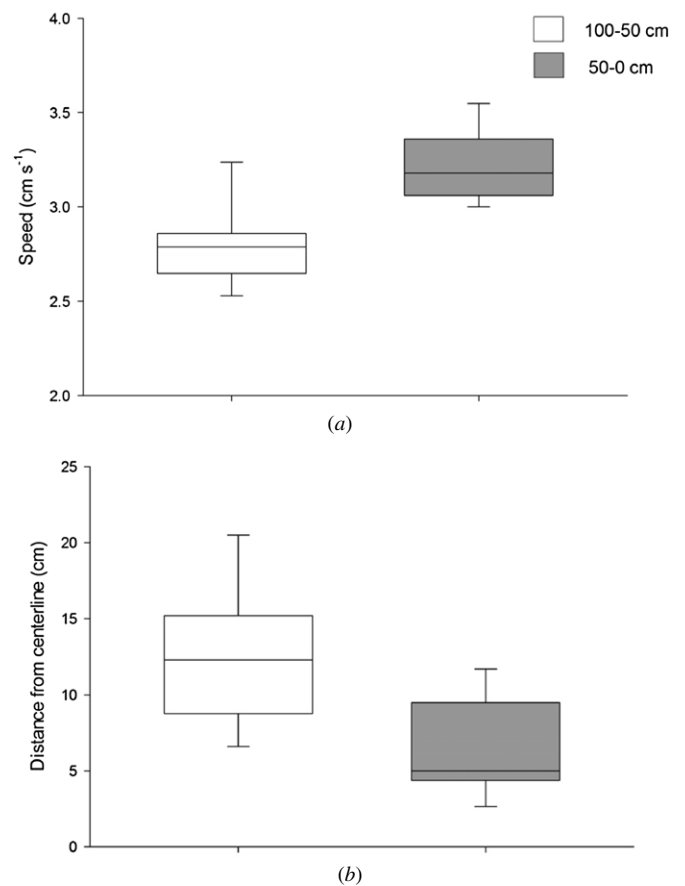


Figure 11. (a) Speed and (b) distance from centerline for successful sensor-mediated tracks. Box plots show mean, quartiles, and 95% confidence limits when the tracker is in the range of 100–50 and 50–0 cm downstream from the odorant source. Both speed and distance from centerline differ significantly as a function of downstream distance (paired $t > 5.0$, $p < 0.001$, $df = 16$ for both comparisons).

6. Discussion

6.1. Comparison to blue crab tracking behavior

Both success rate and movement patterns of the tracker compare favorably to that of blue crabs searching for odorant plume sources in experiments where both odorant release and flow properties are similar. The success rate for blue crabs in comparable plume conditions is 40–85%, with NGDR in the range of 0.5–0.8 (Keller *et al* 2003, Jackson *et al* 2007), placing the performance of the algorithm clearly in the range of animal performance. Our stopping criterion is similar to that used in blue crab studies, where success is declared when an animal is within a body length (about 10 cm) of the source. At this distance, blue crabs appear to switch to a different sensory strategy and actively wave their chelae or probe the substrate in an attempt to contact the source (Weissburg, pers. obs). Like the tracker, movement speed in animals is regulated by odorant pulse arrival rate, and the speed of animals tends to be higher closer towards the source (Page *et al* 2011a), although blue crabs slow down very close to the source. Here differences between the algorithm and blue crab processing strategies may be important; crabs seem to slow down in a graded fashion to

high frequency arrival of odorant spikes close to the source, whereas we implemented a much simpler rule to stop when odorant spike arrival rate exceeded 2 Hz. The path efficiency is high for the tracker (NGDR = 0.7 ± 0.03 , mean \pm std. err.) and blue crabs (NGDR = 0.5–0.8), which indicates that the use of bilateral signal contrast results in the searcher straddling the edge of the odorant plume (Zimmer-Faust *et al* 1995, Keller *et al* 2003, Jackson *et al* 2007) such that the track converges on the plume centerline as the plume narrows towards the source. Interestingly, the distances from the centerline we report here for the tracker are strikingly similar (within 1–1.5 cm) to that reported for blue crabs (Keller *et al* 2003). Movement speed is one aspect of tracker performance that differs substantially from that of blue crabs. Blue crabs maintain average speeds of 10 cm s^{-1} or greater, and are able to complete this search task in 15–20 s. Our autonomous tracker spends substantial time motionless as it samples the plume, and it may be that the vastly more numerous sensors on blue crabs allow for parallel processing that eliminates the need to acquire data for several seconds before moving. Note also that our evaluation of algorithm performance is in one of the least challenging environments for blue crabs (although similar to common test conditions for other similarly sized autonomous agents), and we may see additional performance divergence in environmental conditions of greater spatial and temporal intermittence.

Our hypotheses about sensory processing strategies used by blue crabs to track turbulent plumes produce crab-like behavior when implemented algorithmically. This suggests not only that understanding of blue crabs navigational methods may help us to recreate such abilities in autonomous agents, but that our understanding of the underlying mechanisms used by blue crabs is, at least, somewhat accurate. Although consistency between the behavior of animals and artificial agents using hypothesized animal strategies is not direct evidence, it is at least, the next logical step in a sequence that begins with analysis of behavior in response to specific sensory stimuli. This is a largely correlative enterprise, whereas the failure to reproduce animal-like movement patterns when employing animal inspired strategies would suggest insufficient understanding of what animals actually do.

6.2. Relation to previous design efforts

In past 15 years there has been substantial interest in developing and implementing chemical plume tracking strategies and algorithms. The approaches range from simple reactive movement (Kazadi *et al* 2000) to multiple sensory modalities (e.g., vision and chemical sensing; Ishida *et al* 2006) to creating maps of the probable source location (Lilienthal and Duckett 2004, Pang and Farrell 2006, Kowadlo and Russell 2006) to coordinated sensory acquisition via multiple agents (Hayes *et al* 2002, 2003, Masson *et al* 2009) to mimicking specific organism behavior (e.g., Kuwana and Shimoyama 1998, Grasso *et al* 1996, 1998, 2000). In general, the approaches with the best documented success at the difficult challenge of tracking a turbulent chemical plume are

based on observations of organism behavior. In this section, we discuss the algorithm presented herein in relation to other recent efforts.

Most chemical plume tracking strategies focus on airborne plumes and are inspired by behavior of moths or related organisms. The primary examples of chemical plume tracking in water environments are the lobster-inspired robot design by (Grasso *et al* 1996, 1998, 2000, Grasso and Atema 2002) and the autonomous underwater vehicle (AUV) effort of (Farrell *et al* 2003, 2005). The studies of Grasso *et al* are at roughly the same scale of the current effort (a few meters or less), whereas the AUV effort is at a much larger scale (hundreds of meters). Due to the spatial scale difference, Li *et al* (2001) discuss the applicability of algorithms that are based on moth behavior for AUV guidance, rather than an aquatic-based organism. A major difference between the air and water environments is the diffusivity of the chemical compounds that define odorant plumes, where the diffusivity is typically much greater in the air environment (Webster 2007). Therefore, odorant filaments have sharper boundaries in water compared to those in the air. Nevertheless, many basic elements of autonomous tracking algorithms may be valid in both fluid environments.

Few reported algorithms incorporate the concentration signal structure into the algorithm, and, in fact, many of the sensors and sensor arrangements act to filter the temporal variation of the concentration signal. A common approach is to trigger behavior based on acquiring a suprathreshold concentration signal (e.g., Li *et al* 2001, Harvey *et al* 2008, Sousa *et al* 2008). Farrell *et al* (2003) and Pang and Farrell (2006) report that a binary signal (effectively presence or absence of chemical) is sufficient in their AUV application. Grasso *et al* (1996, 1998, 2000) also employed a suprathreshold approach to induce forward movement. They augmented this approach with directing backward motion when the signal falls below a fixed threshold, which resulted in improved performance by helping the robot to maintain contact with the plume. In contrast to these examples, four studies report use of the temporal or spatial variation in tracking decisions. First, Ishida *et al* (1999) extracted the local spatial directionality of the plume structure via an array of four sensors in order to direct movement of the tracker. Second, Marques *et al* (2002) also estimated the local concentration gradient to direct the robot movement. Third, Ishida *et al* (2005) employed relative changes in the concentration at each sensor with the primary motivation to overcome the slow recovery time of gas sensors. Fourth, Lo Iacono (2010) reports use of concentration variation and the rate of odorant patch encounters in simulations of plume tracking, which highlights the advantage of detecting the edge of odorant filaments. In the current study, the algorithm extracts specific information about the plume structure, namely supra-threshold spikes of concentration, to mediate along-stream motion. Importantly, the threshold is adaptive via calculating a running average of the spike concentration. Further, one sensor, namely the centered and elevated sensor, is given preferential weighting for controlling along-stream motion because it is optimally located to collect the requisite information upon which upstream motion is based. Each of these features appears

unique in comparison to previous studies and follows directly from our detailed observations of blue crab behavior.

Several previous efforts at autonomous plume tracking have employed endogenous counter-turning strategies, which are largely inspired by observed moth behavior. The endogenous counter-turning strategy has been employed in several forms in simulations (Belanger and Arbas 1998, Balkovsky and Shraiman 2002, Lo Iacono 2010), a robotic gantry apparatus (Rutkowski *et al* 2004, Edwards *et al* 2005), and mobile robots (Marques *et al* 2002, Harvey *et al* 2008) with varying degrees of performance. The current strategy does not employ an endogenous counter-turning mechanism since substrate bound creatures, such as blue crabs and lobsters, typically do not operate in this manner (Devine and Atema 1982, Weissburg and Zimmer-Faust 1994). This highlights an important difference between benthic searchers who can stop or reverse direction on the substrate in order to collect more information. In contrast, moths and other airborne searchers continually fly, although we note that moths can fly downstream as a component of casting behavior (e.g., Baker and Haynes 1987).

In contrast to an endogenous counter-turning strategy, many reported algorithms employ steering or heading adjustment based on a bilateral comparison of concentration signal. Typically, the strategy is similar to that reported here, and is to rotate (Kuwana and Shimoyama 1998, Hugues *et al* 2003, Russell *et al* 2003, Lytridis *et al* 2006), translate (Weissburg and Dusenbery 2002, Ishida *et al* 2005), or cast (Grasso and Atema 2002) in the direction of greater concentration stimulus. Martinez *et al* (2006) incorporated an adaptive aspect to the bilateral steering by mediating turn speed based on the concentration sampling history. Further, Grasso *et al* (2000) demonstrated that sensor separation directly influences the straightness of the track. One new aspect of our approach is that we placed the bilaterally-separated sensors closer to the bed (figure 6) in order to mimic the morphology of the blue crab sensor locations that regulate steering (and are located in such a way as to maximize the value of information required for this task). Further, the bilateral spacing of the sensors was selected based on the morphology of blue crabs, which appear to be matched to the cross-stream length scales of plumes typical of turbulent odorant plumes in non-wavy flows (Jackson *et al* 2007). In the context of the results of Grasso *et al* (2000), this may explain why the track shapes are reminiscent of tracks of blue crabs (figures 9 and 10). Our algorithm also allows for simultaneous cross-stream and along-stream movements, which results in diagonal steps (observed in figure 9). The results are consistent with the simulations of Weissburg and Dusenbery (2002) who demonstrated that a simple rule-based algorithm with weighted combination of odor-gated-rheotaxis and chemo-tropotaxis (i.e. cross-stream position adjustment based on spatial comparison of chemical signals) produces behavior consistent with observed blue crab movements to the source.

Our approach relies heavily on the use of memory, which is incorporated by calculating a running average of the spike concentration in order to adaptively adjust the threshold for spike identification. Further, spike characteristics

are compared to the predicted value based on previous samples in order to mediate along-stream motion. The ability to adaptively adjust thresholds is critical for navigating in turbulent plumes where spatial and temporal variation results in different signal environments even under nominally similar release and flow conditions. Nevertheless, only a handful of previous robotic designs have incorporated memory into the tracking algorithm. Kuwana and Shimoyama (1998), for instance, describe a simple memory-based strategy achieved by weighting of neural connections. Martinez *et al* (2006) incorporated adaptive turning based on concentration history. In another example, Porter and Vasquez (2006) integrated memory into their simulations of AUV navigation in order to improve success rate of locating the source location. Again our approach appears effective because it is inspired by direct observations of blue crab behavior.

Finally, a handful of previous efforts have implemented various approaches to the difficult task of autonomous declaration of the source location. Grasso and Atema (2002), for instance, declared the source location when the robot received signal at the bottom sensor for greater than 90% of the sampling period. They report only 6 of 36 tracks with a successful source detection and numerous false positive and false negatives. Farrell *et al* (2003) (and later refined by Li *et al* 2006a, 2006b, 2006c) report a declaration accuracy of 13 m (for tracks starting 975 m from source) based on a scheme that declared that the AUV had reached the source if the farthest upstream locations with concentration signal are clustered within a specified small area. Finally, Li *et al* (2011) declared the source location if the estimated source location based on a particle filter model converge to within a small area and report a source declaration error of 29 cm within a 10 m \times 10 m search arena. The current algorithm presents a novel approach based on exceeding a threshold frequency of concentration spikes, and thus the stopping criterion is mediated by a specific aspect of the plume structure. Again, this approach was inspired directly from observations of blue crab behavior, and the trials presented herein indicate that the approach is successful. It would be a relatively simple extension to make the stopping criterion adaptive in the same way that we have implemented adaptive spike encoding to maintain upstream progress.

7. Conclusions

The summary conclusion based on the trials is that adaptive responses allow for a set of simple rules to be used in a situation-dependent manner to successfully track to a near source location. It is satisfying that the tracking trials demonstrated a high degree of success. With roughly 80% of the trials stopping near the source location, it is clear that the basic elements of the biologically-inspired algorithm design are working effectively. In particular, the implementation of the binary response to supra-threshold signal (to induce along-stream movement) appears to yield sensory-mediated tracking behavior that is consistent with blue crab behavior. The initial threshold is based on the plume-specific parameters far from the source and is updated (using measured spikes) as the tracker

moves forward in order to account for the tendency of the concentration spikes to increase. Thus, the strategy is robust to changing environmental conditions since the determination of what represents a salient stimulus (e.g., chemical spike) is contingent on local information. Further, the bilateral steering aspects of the algorithm also appear very effective at centering the tracker on the plume structure. The trials reveal that the algorithm is highly robust to changing environmental conditions without the need to fine tune the response thresholds a priori since the appropriate thresholds are extracted from the signal itself.

Source location percentage for the tracker compares favorably to blue crab performance. While the tracking period is fairly rapid (roughly 55 s after the initial full cross-stream sweep), it still is much longer than that displayed by blue crabs, which require only about 15–20 s to track a similar distance. Hence, there is significant room for improved performance. Specific features of the algorithm that we plan to implement include adaptive response to the stimulus, including situation-dependent speed and acceleration. Additional features for future development include adaptive specification of the bilateral contrast threshold and adaptive specification of the threshold frequency for autonomous source declaration. These features specifically involve adding neuroadaptive learning to the *decision unit* element.

Acknowledgments

This research was supported by the Defense Advanced Research Projects Agency (DARPA) via award number HR0011-10-1-0063. The authors gratefully acknowledge the preliminary laboratory contribution of Robert Ussery. Thanks also to Shikha Rahman for data collected associated with figures 2–4.

References

- Balkovsky E and Shraiman B I 2002 Olfactory search at high reynolds number *Proc. Natl Acad. Sci.* **99** 12589–93
- Baker T C and Haynes K F 1987 Manoeuvres used by flying male oriental fruit moths to relocate a sex pheromone plume in an experimentally shifted wind-field *Physiol. Entomol.* **12** 263–79
- Belanger J H and Arbas E A 1998 Behavioral strategies underlying pheromone-modulated flight in moths: Lessons from simulation studies *J. Comp. Physiol. A* **183** 345–60
- Breithaupt T and Thiel M 2011 *Chemical Communication in Crustaceans* (New York: Springer)
- Crimaldi J P, Wiley M B and Koseff J R 2002 The relationship between mean and instantaneous structure in turbulent passive scalar plumes *J. Turbulence* **3** 1–24
- Devine D V and Atema J 1982 Function of chemoreceptor organs in spatial orientation of the lobster, *Homarus americanus*: differences and overlap *Biol. Bull.* **163** 144–53
- Dickman B D, Webster D R, Page J L and Weissburg M J 2009 Three-dimensional odorant concentration measurements around actively tracking blue crabs *Limnol. Oceanogr. Methods* **7** 96–108
- Edwards S, Rutkowski A J, Quinn R D and Willis M A 2005 Moth-inspired plume tracking strategies in three-dimensions *IEEE Int. Conf. on Robotics and Automation (Barcelona, Spain)* pp 1669–74
- Farrell J A, Li W, Pang S and Arrieta R 2003 Chemical plume tracing experimental results with a REMUS AUV *MTS/IEEE Conf. on Celebrating the Past—Teaming Toward the Future (San Diego, CA)* pp 962–8
- Farrell J A, Pang S and Li W 2005 Chemical plume tracing via an autonomous underwater vehicle *IEEE J. Ocean. Eng.* **30** 428–42
- Gardiner J M and Atema J 2007 Sharks need the lateral line to locate odor sources: rheotaxis and eddy chemotaxis *J. Exp. Biol.* **210** 1925–34
- Grasso F, Basil J A and Atema J 1998 Toward the convergence: Robot and lobster perspectives of tracking odors to their source in the turbulent marine environment *IEEE/ISIC/CIRA/ISAS Joint Conf. (Gaithersburg, MD)* pp 259–64
- Grasso F, Consi T R, Mountain D and Atema J 1996 Locating odor sources in turbulence with a lobster inspired robot *4th Int. Conf. on Simulation of Adaptive Behavior (Cape Cod, MA)* pp 104–12
- Grasso F W and Atema J 2002 Integration of flow and chemical sensing for guidance of autonomous marine robots in turbulent flows *Environ. Fluid Mech.* **2** 95–114
- Grasso F W, Consi T R, Mountain D C and Atema J 2000 Biomimetic robot lobster performs chemo-orientation in turbulence using a pair of spatially separated sensors: progress and challenges *Robot. Auton. Syst.* **30** 115–31
- Harvey D J, Lu T-F and Keller M A 2008 Comparing insect-inspired chemical plume tracking algorithms using a mobile robot *IEEE Trans. Robot.* **24** 307–17
- Hayes A T, Martinoli A and Goodman R M 2002 Distributed odor source localization *IEEE Sens. J.* **2** 260–71
- Hayes A T, Martinoli A and Goodman R M 2003 Swarm robotic odor localization: off-line optimization and validation with real robots *Robotica* **21** 427–41
- Hugues E, Rochel O and Martinez D 2003 Navigation strategies for a robot in a turbulent odor plume using bilateral comparison *11th Int. Conf. on Advanced Robotics (Coimbra, Portugal)* pp 381–6
- Ishida H, Kobayashi A, Nakamoto T and Moriizumi T 1999 Three-dimensional odor compass *IEEE Trans. Robot. Autom.* **15** 100–6
- Ishida H, Nakayama G, Nakamoto T and Moriizumi T 2005 Controlling a gas/odor plume-tracking robot based on transient responses of gas sensors *IEEE Sens. J.* **5** 537–45
- Ishida H, Tanaka H, Taniguchi H and Moriizumi T 2006 Mobile robot navigation using vision and olfaction to search for a gas/odor source *Auton. Robot.* **20** 231–8
- Jackson J L, Webster D R, Rahman S and Weissburg M J 2007 Bed roughness effects on boundary-layer turbulence and consequences for odor tracking behavior of blue crabs (*Callinectes sapidus*) *Limnol. Oceanogr.* **52** 1883–97
- Kazadi S, Goodman R, Tsikata D, Green D and Lin H 2000 An autonomous water vapor plume tracking robot using passive resistive polymer sensors *Auton. Robot.* **9** 175–88
- Keller T A, Powell I and Weissburg M J 2003 Role of olfactory appendages in chemically mediated orientation of blue crabs *Mar. Ecol. Prog. Ser.* **261** 217–31
- Kowadlo G and Russell R A 2006 Using naive physics for odor localization in a cluttered indoor environment *Auton. Robot.* **20** 215–30
- Kowadlo G and Russell R A 2008 Robot odor localization: a taxonomy and survey *Int. J. Robot. Res.* **27** 869–94
- Kozlowski C, Voigt R and Moore P A 2003 Changes in odour intermittency influence the success and search behaviour during orientation in the crayfish (*Orconectes rusticus*) *Mar. Freshw. Behav. Physiol.* **36** 97–110
- Kuwana Y and Shimoyama I 1998 A pheromone-guided mobile robot that behaves like a silkworm moth with living antennae as pheromone sensors *Int. J. Robot. Res.* **17** 924–33
- Li J-G, Meng Q-H, Wang Y and Zeng M 2011 Odor source localization using a mobile robot in outdoor airflow

- environments with a particle filter algorithm *Auton. Robot.* **30** 281–91
- Li W, Elgassier M M, Bloomquist C and Srivastava K 2006a Multisensor integration for declaring the odor source of a plume in turbulent fluid-advected environments *IEEE/RSJ Int. Conf. on Intelligent Robots and Syst. (Beijing, China)* pp 5534–39
- Li W, Elgassier M M, Rutledge T and Sutton J 2006b Design of source identification zones for declaring an odor source in turbulent fluid-advected environments *IEEE Int. Conf. on Information Reuse and Integration (Waikoloa, HI)* pp 466–71
- Li W, Farrell J A and Cardé R T 2001 Tracking of fluid-advected odor plumes: Strategies inspired by insect orientation to pheromone *Adapt. Behav.* **9** 143–70
- Li W, Farrell J A, Pang S and Arrieta R 2006c Moth-inspired chemical plume tracing on an autonomous underwater vehicle *IEEE Trans. Robot.* **22** 292–307
- Lilienthal A and Duckett T 2004 Building gas concentration gridmaps with a mobile robot *Robot. Auton. Syst.* **48** 3–16
- Lilienthal A, Loutfi A and Duckett T 2006 Airbourne chemical sensing with mobile robots *Sensors* **6** 1616–78
- Lo Iacono G 2010 A comparison of different searching strategies to locate sources of odor in turbulent flows *Adapt. Behav.* **18** 155–70
- Lytiridis C, Kadar E E and Virk G S 2006 A systematic approach to the problem of odour source localisation *Auton. Robot.* **20** 261–76
- Marques L, Nunes U and de Almeida A T 2002 Olfactory-based mobile robot navigation *Thin Solid Films* **418** 51–8
- Martinez D, Rochel O and Hugues E 2006 A biomimetic robot for tracking specific odors in turbulent plumes *Auton. Robot.* **20** 185–95
- Masson J-B, Bechet M B and Vergassola M 2009 Chasing information to search in random environments *J. Phys. A: Math. Theor.* **42** 434009
- Nakamoto T, Ishida H and Moriizumi T 1999 A sensing system for odor plumes *Anal. Chem.* **4** 531A-7A
- Page J L, Dickman B D, Webster D R and Weissburg M J 2011a Getting ahead: context-dependent responses to odor filaments drives along-stream progress during odor tracking in blue crabs *J. Exp. Biol.* **214** 1498–512
- Page J L, Dickman B D, Webster D R and Weissburg M J 2011b Staying the course: chemical signal spatial properties and concentration mediate cross-stream motion in turbulent plumes *J. Exp. Biol.* **214** 1513–22
- Pang S and Farrell J A 2006 Chemical plume source localization *IEEE Trans. Syst. Man Cybern. B* **36** 1068–80
- Porter M J and Vasquez J R 2006 Bio-inspired, odor-based navigation *Proc. SPIE* **6228** 62280V
- Rahman S and Webster D R 2005 The effect of bed roughness on scalar fluctuations in turbulent boundary layers *Exp. Fluids* **38** 372–84
- Reidenbach M A and Koehl M A R 2011 The spatial and temporal patterns of odors sampled by lobsters and crabs in a turbulent plume *J. Exp. Biol.* **214** 3128–53
- Russell R A 2001 Survey of robotic applications for odor-sensing technology *Int. J. Robot. Res.* **20** 144–62
- Russell R A, Bab-Hadiashar A, Shepherd R L and Wallace G G 2003 A comparison of reactive robot chemotaxis algorithms *Robot. Auton. Syst.* **45** 83–97
- Rutkowski A J, Edwards S, Willis M A, Quinn R D and Causey G C 2004 A robotic platform for testing moth-inspired plume tracking strategies *IEEE Int. Conf. on Robotics and Automation (New Orleans, LA)* pp 3319–24
- Sousa P, Marques L and de Almeida A T 2008 Toward chemical-trail following robots *7th Int. Conf. on Machine Learning and Applications (San Diego, CA)* pp 489–94
- Vickers N J 2000 Mechanisms of animal navigation in odor plumes *Biol. Bull.* **198** 203–12
- Webster D R 2007 Trace chemical sensing of explosives *The Structure of Turbulent Chemical Plumes* ed R L Woodfin (Hoboken, NJ: Wiley-Interscience) chapter 5 pp 109–29
- Webster D R, Rahman S and Dasi L P 2003 Laser-induced fluorescence measurements of a turbulent plume *ASCE J. Eng. Mech.* **129** 1130–7
- Webster D R and Weissburg M J 2001 Chemosensory guidance cues in a turbulent chemical odor plume *Limnol. Oceanogr.* **46** 1034–47
- Webster D R and Weissburg M J 2009 The hydrodynamics of chemical cues among aquatic organisms *Annu. Rev. Fluid Mech.* **41** 73–90
- Weissburg M J and Dusenbery D B 2002 Behavioral observations and computer simulations of blue crab movement to a chemical source in a controlled turbulent flow *J. Exp. Biol.* **205** 3387–98
- Weissburg M J and Zimmer-Faust R K 1994 Odor plumes and how blue crabs use them in finding prey *J. Exp. Biol.* **197** 349–75
- Zimmer-Faust R K, Finelli C M, Pentcheff N D and Wethey D S 1995 Odor plumes and animal navigation in turbulent water flow. A field study *Biol. Bull.* **188** 111–6